Catalysis Science & Technology

PAPER

View Article Online
View Journal | View Issue

Cite this: *Catal. Sci. Technol.*, 2014, 4, 1357

Dehydration of xylose and glucose to furan derivatives using bifunctional partially hydroxylated MgF_2 catalysts and N_2-stripping†

I. Agirrezabal-Telleria,*[a] Y. Guo,[b] F. Hemmann,[c] P. L. Arias[a] and E. Kemnitz[b]

Received 31st January 2014,
Accepted 11th February 2014

DOI: 10.1039/c4cy00129j

www.rsc.org/catalysis

The current furfural production yield is low due to the use of non-selective homogeneous catalysts and expensive separation. In this work, partially hydroxylated MgF_2 catalysts, synthesized using different water contents, were screened during xylose dehydration in water–toluene at 160 °C. The different Lewis/Brønsted ratios on the MgF_2 catalysts showed that under-coordinated Mg can isomerize xylose to xylulose, whilst the surface OH-groups were responsible for the dehydration reactions. The presence of glucose as a co-carbohydrate reduced the furfural selectivity from 86 to 81%, whilst it also led to high 5-hydroxymethylfurfural selectivity. The tests catalyzed by MgF_2 in combination with simultaneous N_2-stripping showed that a furfural selectivity of 87% could be achieved using low xylose loadings. Moreover, the catalysts regenerated by H_2O_2 showed high activity during the dehydration tests in water–toluene at 160 °C.

1. Introduction

In the past years, several environmental and economic issues related to petroleum-derived fuels and chemicals have arisen, so the interest for the design of biorefineries and the research related to novel catalytic systems has renewed.[1] In this sense, second generation fuels can directly affect the feasibility of integrated strategies to use lignocellulosic wastes as bio-based product sources. Given the high oxygen content of biomass derived carbohydrates, a key process to efficiently reduce it is by dehydration, operating in aqueous phase. Among furan-based chemicals, furfural (FUR) is a widely used chemical for applications as an industrial solvent or precursor for high value-added products. FUR is industrially produced from pentosan-rich biomass (bagasse or corncob) *via* xylose cyclodehydration, obtaining low FUR yields (50%).[2] Three main issues appear in the manufacturing processes of biomass-derived furfural:

1. The use of homogeneous H_2SO_4 type catalysts, increasing the corrosion and separation issues, as well as achieving low furfural selectivity.

2. The separation technology is based on steam, showing high energy requirements for its production and diluting the stripped stream, which increases the subsequent distillation costs.[3]

3. The furfural production technologies are limited to the upgrading of the hemicellulose in the biomass. In this sense, interesting and feasible routes, such as the glucose dehydration reactions to 5-hydroxymethylfurfural (HMF), are required.

For these reasons, the development of an appropriate catalyst design and sustainable chemical technologies remains of great interest for the growth of furan-based industry.

Among the novel catalysts, most of the recent publications aimed to maximize FUR production by using heterogeneous catalysts and biphasic water–organic solvent systems[4] or ionic-liquids.[5] The studied materials featured suitable textural and acid-site properties to reduce FUR degradation reactions and thus increase the FUR selectivity.[6] Valente and co-workers synthesized and tested several catalysts, ranging from sulfated zirconia,[7] acidic cesium salts[8] and functionalized micro/mesoporous catalysts.[9] Other studies focused on the use of zeolitic structures,[10,11] metal oxides[12] or sulfonated silica-shells,[13] showing high FUR yields.

In most of the studies, the reaction was catalyzed by Brønsted sites. The mechanism of this reaction has been mostly studied under the presence of heterogeneous[4] or homogeneous[3,14] Brønsted (B) acid-sites. According to the proposed mechanism, Brønsted sites shift the reaction to convert xylose to furfural without any intermediate.[15] Recently, the catalytic activity of different heterogeneous/homogeneous Lewis (L) and Brønsted acids,[16] SAPO[17] and BEA-TUD[18] was

[a] *Department of Chemical and Environmental Engineering, Engineering School of the University of the Basque Country (UPV/EHU), Alameda Urquijo s/n, 48013, Bilbao, Spain. E-mail: iker.aguirrezabal@ehu.es; Fax: +34 946014179; Tel: +34 617912295*
[b] *Institut für Chemie, Humboldt-Universität zu Berlin, Brook-Taylor Straße 2, D-12489, Berlin, Germany*
[c] *BAM Federal Institute for Materials Research and Testing, Division 1, Richard Willstaetter Straße 11, D-12489, Berlin, Germany*
† Electronic supplementary information (ESI) available. See DOI: 10.1039/c4cy00129j

also reported. Among the catalysts used for carbohydrate conversion, Lewis acid-sites have been mainly applied to upgrade the glucose sugar as feed-source to achieve high HMF yields *via* its fructose isomer.[1,19,20] It is worth noting that some of the different types of Lewis sites might be transformed to Brønsted under the presence of water. In this sense, the acid properties and their nature play an important and complex role when correlating them to the catalytic carbohydrate conversion activity and to the reaction mechanism. In summary, the Lewis/Brønsted surface properties showed high relevance in order to design suitable catalysts to produce furfural.

Among the catalysts featuring bifunctional properties, partially hydroxylated MgF_2 catalysts showed interesting properties to study carbohydrate dehydration type reactions, especially due to the tunable Lewis/Brønsted ratios.[21] According to the pyridine adsorption results, the under coordinated Mg^{2+} ions were responsible for the Lewis acidity, whereas the surface hydroxyl groups showed high Brønsted acidity.[22,23] During the study of the glycerol acetylation catalytic activity, the authors found an optimum L/B ratio to maximize the production of diacetyl and triacetylglycerol. The Brønsted acidity could be modified using different fluorosulfonic precursors under different grafting conditions.[24] In this way, tunable L/B ratios were achieved. These types of bifunctional catalysts show interesting applications to study the reaction mechanism and catalytic activity of xylose dehydration. In order to optimize the FUR yield, the competition between dehydration and degradation reactions could be controlled by varying the L/B ratios. In order to exploit the biggest fraction of the carbohydrate fraction in the biomass, glucose upgrading routes are required. However, it has to be taken into account that the use of glucose in xylose feed could considerably reduce the furfural production yield due to enhanced secondary reactions.

According to published reports, the carbohydrate conversion catalytic field can be properly studied under water–toluene biphasic batch conditions.[26] However, the industrial application of such conditions would increase solvent–furfural separation and purification costs. For this reason, novel technologies using advanced separation systems, such as easily recyclable solvents, under mixed carbohydrate contents would be advisable. Recent studies focused on reactions in aqueous phase operating at high temperature[25] or using different stripping agents such as N_2, showing significant FUR yield improvement.[26] These conditions allowed stripping of the FUR from the reaction medium at high selectivity, allowing an easier stripping agent–water separation and reducing further FUR purification stages. In order to apply the new separation techniques at the industrial scale, more realistic reaction mixtures must be studied including not only xylose but also sugars derived from lignocellulosic biomass, such as glucose. In this way, a complete upgrading route of a big fraction of the hemicellulosic–cellulosic fraction of biomass could be achieved. In order to achieve higher isomerization and dehydration reactions of xylose and glucose type molecules, bifunctional partially hydroxylated MgF_2 catalysts combined with novel separation processes seem an alternative as previously reported.[27] In summary, this work aims to find a solution to the catalytic and technological issues of the furfural manufacturing process, as well as to go beyond the current state-of-the-art studying of the aspects previously mentioned:

1. Finding new alternatives in the catalysis field using bifunctional MgF_2 catalysts to produce FUR under batch conditions. The tuning of their properties allows control of the simultaneous dehydration and side-reactions (Scheme 1).

2. Using a novel FUR separation technology, such as the semi-continuous N_2-stripping approach, combined with more selective heterogeneous catalysts than previously reported.[27]

3. The combination of such concepts using more realistic feed than reported,[24] including glucose. Given the Lewis + Brønsted nature of the partially hydroxylated MgF_2 catalysts, not only FUR but also HMF could be simultaneously produced. Moreover, the catalyst stability and regeneration tests will prove the potential of such heterogeneous systems to upgrade hemicellulose–cellulose type biomass to interesting molecules. This would provide an alternative route to the current FUR manufacturing catalysis and technology.

2. Materials and methods

2.1 Catalyst preparation

The partially hydroxylated MgF_2 catalysts were synthesized using metallic Mg and the fluorolytic sol–gel process: Mg (Aldrich, 99.98%) (7.8 g, 325 mmol) was first dissolved in dried methanol (400 mL) at room temperature overnight. After complete Mg dissolution, the corresponding methanolic HF amount (650 mmol) was added at room temperature. The MgF_2 catalyst series were prepared using four different HF concentrations (40, 57, 71 and 87 wt.%, calculated as $m_{HF}/(m_{HF} + m_{water})$). The 40 and 71 wt.% solutions were commercially purchased from Fluka and Sigma-Aldrich, respectively. The 57 and 87% solutions were prepared right before addition. These concentrations correspond to the HF

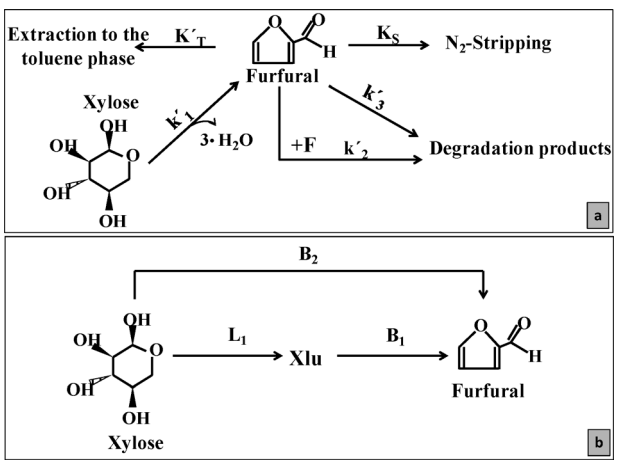

Scheme 1 The kinetic and diffusion constants during xylose dehydration to furfural (a). Mechanism and reaction pathways using Lewis and Brønsted catalysts during the dehydration of xylose in water (b).

concentrations (wt.%) in the solution to be added to the dissolved Mg. The catalyst, as an example of a HF concentration of 40%, was denoted as M-40. After the addition of HF, the mixtures were vigorously stirred and reacted to form highly viscous transparent sols. These were aged at room temperature overnight, dried under vacuum at increasing temperature until 100 °C for 3 h and maintained at this temperature for 2 h.

2.2 Catalyst characterization

2.2.1 General properties. The surface properties of the samples were determined by acquiring N_2 adsorption–desorption isotherms at 77 K and on Micromeritics ASAP 2020 equipment. Samples were first degassed under vacuum at 100 °C. Surface areas were calculated according to the BET method. The X-ray powder diffraction (XRD) patterns were recorded in the 2θ range of 5–60° (step width 0.5°, 100 s per step) using a XRD-7 Seifert-FPM diffractometer with a CuKα radiation source. The samples were prepared for flat plates. The TG-MS thermal analysis experiments were performed on a Netzsch STA 409C apparatus. A DTA-TG sample-holder system (a Pt/PtRh10 thermocouple) was used, and measurements were carried out in a N_2 atmosphere. The thermo analyzer was equipped with a Balzers QMG429 quadrupole mass spectrometer for multiple ion detection modes.

^{19}F MAS NMR spectra were recorded on a Bruker AVANCE 400 spectrometer (Larmor frequency: $\nu_{^{19}F}$ = 376.4 MHz) using a 2.5 mm MAS probe with 2.5 mm rotors made from ZrO_2. The spectra were recorded with a $p/2$ pulse duration of $p1$ = 4.0 μs, a spectrum width of 400 kHz, and a recycle delay of 10 s. Up to 60 rotor periods were added before echo detection in rotor synchronized echo experiments. The isotropic chemical shifts δ_{iso} of ^{19}F resonances are given with respect to the C_6D_6 standard. Existent background signals of ^{19}F were suppressed with the application of a phase-cycled depth pulse sequence.[28]

2.2.2 Surface acid-properties

2.2.2.1 Acid-site qualification. FTIR photoacoustic pyridine adsorption spectroscopy was carried out to qualitatively evaluate the surface acid-sites according to two procedures:

1. Denoted as Pyr-150: the sample (75 mg) was pre-heated at 150 °C under N_2 flow for 15 min and then 60 mL of pyridine were injected at 150 °C into the sample tube. The sample was flushed with nitrogen for additional 15 min to remove physisorbed pyridine. Sample spectra were recorded at room temperature using a MTEC cell and a FTIR system 2000 (Perkin-Elmer). Spectra of the samples without pyridine adsorption were also measured as the background.

2. Denoted as RT-Pyr: the FTIR pyridine adsorption spectroscopy measurements at room temperature (RT-Pyr) were carried out in a Thermo Scientific Nicolet iS10 spectrometer using pressed (10^7 Pa) sample discs. A movable quartz sample holder permits the adjustment of the sample disc in the infrared beam for spectra acquisition. Samples were degassed at 150 °C under high vacuum (2 h). The addition of accurately known pyridine probe doses (at room temperature) was measured by means of a calibrated volume connected to a pressure gauge to control the probe pressure. IR spectra were recorded for each dosing and the pyridine μmol *versus* peak area was plotted.

2.2.2.2 Acid-site quantification. Temperature programmed desorption of ammonia (NH_3-TPD) was carried out as follows: the sample (0.2 g) was first heated under N_2 up to 300 °C and then at 120 °C exposed to NH_3. After flushing the excess NH_3 at 120 °C with N_2 for 1 h and cooling to 80 °C, the TPD program was started (10° min^{-1} up to 500 °C, keeping for 30 min). Desorbed NH_3 was monitored continuously *via* FTIR spectroscopy (Perkin-Elmer).

For the acid quantification measurements using NMR (denoted as Pyr-NMR), 700 mg of the sample were weighted in a Schlenk flask, followed by an activation step at 200 °C under vacuum for 2 h to remove physisorbed water. Then, 30 μl of ^{15}N-pyridine (~367 μmol) were added and the mixture was stirred for 30 min at 150 °C to ensure homogeneous pyridine distribution. Physisorbed pyridine was removed under vacuum at 150 °C for 1 h. Rotors for MAS NMR experiments were carefully filled in the glovebox with a mixture of the sample and NH_4Cl (^{15}N enrichment, 9.5%) in a ratio of 20 : 1. For quantitative investigations, ^{15}N-NMR single pulse experiments with presaturation and ^{1}H–^{15}N CPMAS (cross-polarization with magic angle sample spinning) experiments are necessary, as described elsewhere.[29] ^{15}N MAS NMR single pulse spectra were recorded at a Larmor frequency of 60.8 MHz. The MAS frequency was 6.5 kHz. The ^{15}N 90° pulse length was 6.2 μs. The repetition time in the single pulse spectra was set to 5 s with previous saturation. ^{1}H high power decoupling (TPPM) was applied and 3072 scans were accumulated. ^{15}N chemical shifts (δ) are reported relative to CH_3NO_2 with NH_4Cl as the secondary standard (δ = −341 ppm).[30] The ^{1}H–^{15}N CPMAS experiments are needed for the determination of the T_1 corrections of the time optimized ^{15}N MAS NMR spectra using the Torchia method.[31] The sample spinning frequency was 6.5 kHz and the spectra were recorded using a ^{1}H 90° pulse length of 6.5 μs, a contact time of 2 ms, and a repetition time of 3 s. The ^{15}N spin lock field was held constant while the ^{1}H spin lock field was ramped down to 50% of its initial value. Mostly 4096 scans were accumulated, and high power decoupling (TPPM) was applied.

2.3 Catalytic tests and product analyses

The batch tests were carried out in a high-pressure Teflon lined reactor (BR-500 from Berghof) stirred at 500 rpm. The reactor was first loaded with 0.6 g of the catalyst, 150 mL of water and 150 mL of toluene. In order to keep the reaction medium in liquid-phase, the system pressure was maintained at 15 bar. Once the solution was heated to 160 °C, the corresponding xylose solution was added using a Gilson 305 pump to reach a xylose initial concentration of 20 g L^{-1} of aqueous phase (0.44 M). Reaction samples were taken at different intervals using a needle valve.

The N_2-stripping tests were carried out in a 2 L reactor (Autoclave Engineers), with controlled electric-heating and stirred at 500 rpm (Scheme 1). In a typical SC experiment

operating at 180 °C and 10 bar, the reactor was first loaded with the corresponding amount of MgF_2 catalyst and heated up to 190 °C with deionized water (75% of the total initial reactor volume). The remaining 25% of the total reactor volume was fed from a nitrogen-pressurized vessel (to reach the corresponding initial xylose concentration, X_0). This set-up allowed the feed solution to be held at room temperature until the desired temperature was reached in the reactor to minimize the initial feed degradation. During the N_2-stripping tests, mass-flow controlled nitrogen was bubbled into the liquid bottom at 150 mL min^{-1} (STP). This gas flow stripped the water–furfural vapour stream. The gaseous flow was later fed to a condenser (cooled by the Peltier effect at 10 °C), where gas and liquid streams were separated. The condensate was continuously weighted. Automatic control valves were used to regulate the reactor-pressure and the liquid level in the condenser.

Xylose conversion (X_X) was calculated at different intervals and FUR selectivity (FUR_S) was calculated as the mol of FUR obtained per mol of converted xylose. Glucose conversion (G_X) and HMF selectivity (HMF_S) were calculated in the same manner. In all cases, carbohydrate conversion values were calculated using the sum of reactants in the reactor phase: in the water phase during the water–organic batch tests, and in the reactor during the N_2-stripping tests. Moreover, the FUR_S/HMF_S values in the batch tests were calculated as the sum in the water and organic phase; whilst the FUR_S/HMF_S for the N_2-stripping tests was calculated as the sum of the FUR/HMF present in the reactor and in the condensate. Product yield (FUR_Y or HMF_Y) was calculated as conversion × selectivity.

The carbohydrate content in the reactor was quantified using a HPLC module ICS-3000 from Dionex coupled to an AS40 autosampler. X and G were quantified using a CarboPac PA20 3 × 150 mm column at 30 °C and 0.5 mL min^{-1} using 8 mM of NaOH as the mobile phase. Detection was performed using an electrochemical cell, with integrated amperometry and the Standard Carbohydrate Quad method. FUR and HMF were quantified in a 1260 Infinity module from Agilent. The products were separated in a Zorbax SB-C18 column (3.5 μm, 3.0 × 150 mm) at 1 mL min^{-1} and 35 °C using water as the eluent.

Secondary-products were identified by GC-MS (6890 GC and 5973-Mass Selective Detector from Agilent) using a DB-FFAP column, helium as the carrier gas at 1 mL min^{-1} and an injection volume of 1 μL. The ^1H (νLarmor(^1H) = 400.1 MHz) and ^{13}C (νLarmor(^{13}C) = 100.6 MHz) liquid-NMR spectra of the reaction products were recorded on a Bruker AVANCE II 400 under standard conditions for NMR parameters. All spectra were obtained using the specific signals of deuterated benzene as the reference standard in melted off locked-in tubes.

3. Results and discussion

3.1 Catalyst characterization

According to the reported data,[21] the partially hydroxylated MgF_2 containing different HF concentrations showed L/B ratios from 0.4 to 1.0 (based on the area of the pyridine vibration bands) for M-40 and M-71, respectively. The L/B ratio differences were mainly attributed to the different concentrations of OH groups on the sample surfaces. Troncea *et al.* reported the highest OH content for the M-40 sample, caused by the higher water content in the aqueous HF used for the synthesis.[21]

3.1.1. General properties. The change of the S_{BET} values has been already reported for MgF_2 samples synthesized using HF with different concentrations.[21] The series of the partially hydroxylated MgF_2 catalysts presented typical mesoporous isotherms with H2 hysteresis loops. As observed in Table 1, the presence of different HF concentrations in the xerogel modified the structure of the pure MgF_2 matrix by changing the adsorption–desorption capacity and thus reducing the mesoporous diameter to 25.2 Å and the surface area from ~460 m^2 g^{-1} (for M-87 and M-71) to ~280 m^2 g^{-1} (for M-57 and M-40). Taking into account that the MgF_2 surface area is given by the interparticle voids, the addition of increasing amounts of water created bigger aggregates and thus increased the pore size and reduced the S_{BET}. According to the XRD data, the crystallinity of the MgF_2 materials was barely affected by the HF concentration differences. The catalysts showed the typical reflections of MgF_2[23] (PDF-136895) centered at 27° (110), 40° (111) and 53° (211).

The surface-property differences on the MgF_2 catalysts were also confirmed by solid-state ^{19}F-MAS-NMR measurements. The MgF_2 samples showed a dominant ^{19}F signal centered at δ = −197 ppm, at nearly the same position as that of crystalline MgF_2. During the synthesis of partially hydroxylated MgF_2 samples, the competition between fluorolysis and hydrolysis of $Mg(OCH_3)_2$ was enhanced due to the addition of water on the $MgF_X(OH)_{2-X}$ xerogel. The asymmetric shape and the shifting of the −197 ppm signal were previously attributed to the presence of un-substituted oxygen species on its surface.[23,32] Among the materials prepared here, the presence of abundant OH groups on M-40 shifted the main peak to −196.7 ppm and created a shoulder in the lower field of the spectrum (δ = −179.3 ppm). On the other hand, the presence of minor OH contents on M-71 reduced the asymmetric shape of the −197.4 ppm signal.

According to the TG-MS data, the MgF_2 catalysts showed a very broad exothermal peak in the DTA curves, characteristic of the sol–gel procedure. As depicted in Fig. 1, the M-40 and M-71 catalysts showed an overall weight loss of *circa* 13%, assigned to the loss of strongly bonded water (100–350 °C) and to the OH surface groups (350–500 °C). As observed in the m18 profiles, a considerable increase of the surface OH incorporation for the sol prepared using 40% HF concentration was achieved compared to M-71. Based on the S_{BET} values for each catalyst and assuming that all strongly bonded OH groups were entrapped in the pores, the M-40 sample showed the highest OH surface concentration (0.71 mmol OH m^{-2}). As observed in Fig. 1, the MS signal also detected some other traces corresponding to fluorine (m19) or methanol (m31).

Table 1 Physicochemical properties of partially hydroxylated MgF_2 catalysts and the activity during xylose dehydration in water–toluene at 160 °C in batch

Sample	S_{BET} ($m^2\ g^{-1}$)	Pore (Å)	Pore vol. ($m^3\ g^{-1}$)	Acidity Pyr-NMR[a] ($\mu mol\ g^{-1}$) Total	Lewis	Brønsted	Ratio L/B	NH_3-TPD[b] ($\mu mol\ g^{-1}$)	(TOF × 10^6)[c] $mmol_X\ \mu mol_{ACID}^{-1}\ h^{-1}$	X_X[d] (%)	FUR_S[d] (%)	FUR_Y[d] (%)
M-40	271	27.5	0.19	303	303 ± 45	—	High	450	10.9	82	44	36
M-57	284	27.1	0.17	438	302 ± 34	136	2.2	481	4.5	60	69	41
M-71	460	26.9	0.30	334	258 ± 24	76	3.4	567	6.3	63	86	54
M-87	465	25.2	0.27	308	256 ± 19	52	4.9	645	3.6	35	88	31
M-100	467	23.2	0.27	—	—	—	—	—	—	32	43	14
Amberlyst	<1	—	—	—	—	—	Low	2550	0.8	90	44	39

[a] Acidity of Lewis and Brønsted sites quantified by pyridine adsorption at 150 °C followed by ^{15}N-NMR analysis. [b] Total acidity quantified by NH_3 adsorption followed by TPD up to 550 °C. [c] TOF value calculated on converted xylose after 4 h of reaction and based on Pyr-NMR analyses. [d] Xylose conversion (X_X), FUR selectivity (FUR_S) and yield (FUR_Y) after 8 h.

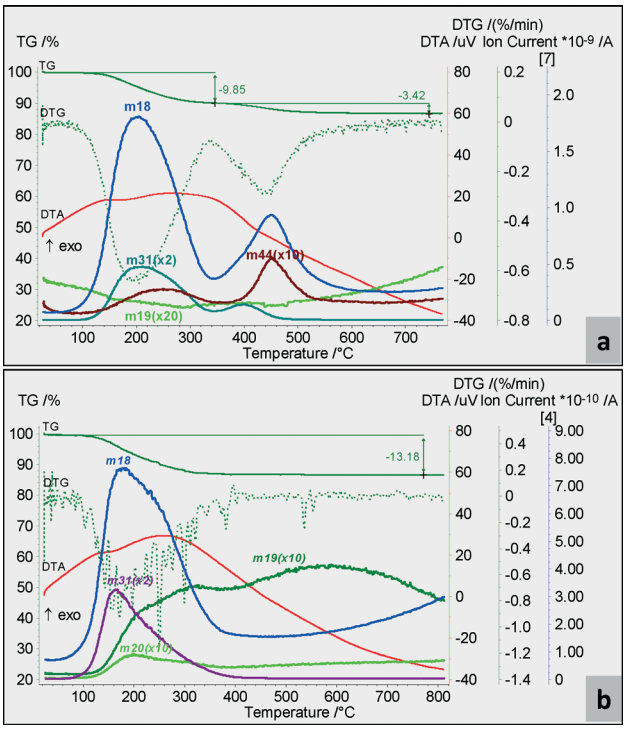

Fig. 1 TG, DTG, DTA and the MS profiles of M-40 (a) and M-71 (b).

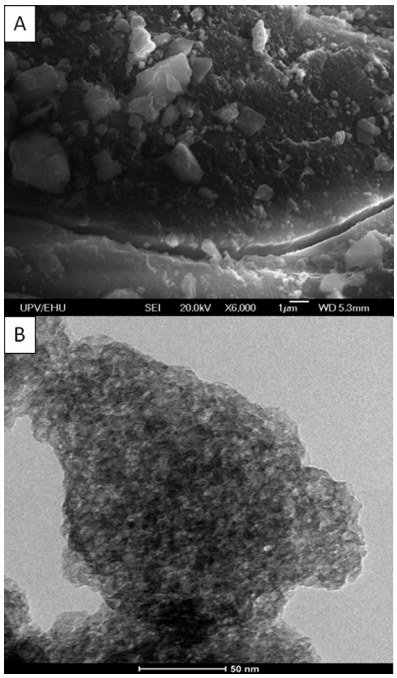

Fig. 2 SEM (A) and TEM (B) images of the partially hydroxylated M-71 fresh sample.

According to the scanning electron microscope picture in Fig. 2A, the M-71 sample, as well as the rest of the catalysts, presented a particle sizes around 0.5–3 m. However, no further information could be extracted from the transmission electron microscope image (Fig. 2B).

3.1.2. Characterization of the surface acidity

3.1.2.1 Acid-site qualification. The qualitative and quantitative analyses of the acidity of heterogeneous catalysts are determined to correlate these properties to the catalytic activity during xylose dehydration to FUR. The acid properties of the catalysts were first qualitatively evaluated adsorbing pyridine at room temperature (RT-Pyr).

According to the RT-Pyr FTIR measurements (not shown), the Lewis sites on all the samples showed high pyridine protonation capacity, whilst just the M-57 Brønsted sites were detected. During these analyses, the pyridine diffusivity and its protonation capacity were considerably reduced, meaning that mainly strong acid-sites were capable of showing pyridine vibration bands. The capacity to protonate Brønsted sites by RT-Pyr (measured by the adsorption peak areas) was as follows: M-40 < M-87 < M-71 < M-57. It seems that a minimum Brønsted-site content or strength was required to detect Brønsted sites using the RT-Pyr technique.

On the other hand, the addition of pyridine at higher temperature (denoted as 150-Pyr) allowed evaluation of nearly the totality of the Lewis or Brønsted acid-types on the catalyst surface by enhancing its diffusion to the acid-site and its protonation for IR detection. As observed in Fig. 3, despite the high OH concentration on the M-40 surface (based on the TG-MS data), it seems that these Brønsted sites were not strong enough to protonate pyridine and even xylose (as it

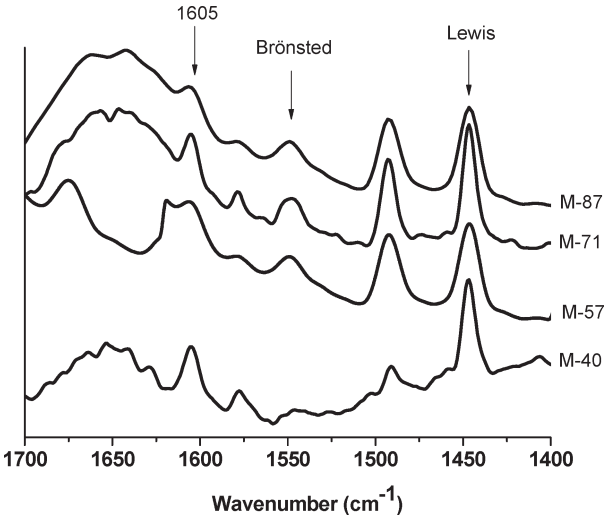

Fig. 3 The FTIR spectra of the M-40 and M-71 samples after pyridine adsorption at 150 °C.

will be discussed later). This can be explained by the following: the M-40 sample contained the highest OH content but lower fluorine than M-71. As usually observed for $Mg(OH)_2$, which is mainly basic, the lower fluorine content on M-40 could also be reflected as lower Brønsted acidity. On the other hand, as observed in Fig. 3, the catalysts with lower OH contents (M-57, M-71, and M-87) showed both Lewis and Brønsted sites in the IR spectra. In other words, although these catalysts had fewer surface OH groups, their Brønsted acidity was stronger than that of the OH-rich sample, M-40.

In general, the shifting (to a higher wavenumber range) of the vibration band at 1605 cm^{-1} states the strength of the Lewis sites. However, this band appeared at the same position in the spectra of all the samples.

3.1.2.2 Acid-site quantification. The pyridine adsorption-IR is a powerful method to study the surface acidity. However, it cannot be used as a quantification method by simply calculating the vibration peak area ratio.[21] The presence of Lewis sites requires the use of these techniques, in order to avoid the quantification errors associated to inactive sites such as in the aqueous-phase titrations.[33] This was already reported on a broad range of Lewis/Brønsted catalysts.[16] For this reason, the total acidity was quantified using two different procedures: pyridine adsorption followed by ^{15}N-NMR (Pyr-NMR) and NH_3 adsorption followed by TPD (NH_3-TPD).

According to the NH_3-TPD data, the fresh MgF_2 samples showed a FTIR intensity for desorbed NH_3 starting at 200 °C and decaying at ~400 °C. As observed in Table 1, the quantification of the total acid sites by NH_3-TPD showed higher values than Pyr-NMR. One possible explanation is that the smaller NH_3 molecule can diffuse and be adsorbed on the acid-sites which are not accessible to pyridine. Moreover, the TPD carried out up to 550 °C ensures that all adsorbed NH_3 is removed, whilst during pyridine adsorption analyses (as observed later) some of the entrapped pyridine may not be quantified. However, taking into account the presence of adsorbed water, the NH_3-TPD analyses showed low reproducibility. Therefore, only Pyr-NMR values will be used for further discussion (explained below). Moreover, Pyr-NMR is the only available analysis to differ the Lewis/Brønsted acid-site quantities on these MgF_2 catalysts.

The Pyr-NMR spectra allowed selective separation of the physisorbed pyridine (centered at −80 ppm), Lewis sites (−100 ppm), Brønsted sites (−174 ppm) and the standard NH_4Cl (−341 ppm). The Pyr-NMR results confirmed the FTIR data previously discussed using the 150-Pyr technique. M-40 showed no Brønsted acidity, proving that the presence of more OH groups on M-40 reduced the pyridine protonation capacity of the Brønsted sites. On the other hand, M-57 showed the highest content of Brønsted acid-sites (136 μmol g^{-1}). In general, the change in the concentration of Brønsted acidity measured by Pyr-NMR showed the same trend as the Lewis acidity (Table 1).

Additionally, the RT-Pyr analyses were attempted to quantify the acid-site content by dosing small quantities of pyridine and recording its IR spectra. The corresponding extinction coefficients were derived for quantification; however, given the low protonation capacity of the Brønsted acid-sites at this temperature, the total values were far below the Pyr-NMR values. This is a powerful method compared to the more sophisticated Pyr-NMR techniques, but not appropriate for these catalysts.

3.2 Catalytic activity during carbohydrate conversion

First of all, and in order to prove the heterogeneous nature of the MgF_2 catalysts, the liquid solution after the reactions at 160 °C was analyzed by means of ^{19}F liquid NMR. As observed in Fig. A1, ESI† the presence of fluorinated compounds is negligible, confirming the heterogeneous nature of the tested catalysts.

3.2.1 Screening and reaction mechanism during xylose dehydration to FUR. A preliminary MgF_2 catalyst screening was carried out in water–toluene at 160 °C in order to correlate the physicochemical properties to the catalytic activity and the reaction mechanism. Even if suitable catalyst screening is not possible at nearly full xylose conversions, the catalytic activities after 20 h of reaction-time showed the same trend as the data in Fig. 4 after 8 h. It is worth mentioning that the xylose dehydration kinetics has been previously correlated to the L/B ratio.[15,16]

As observed in Fig. 4a, M-40 (dominant Lewis acid-sites) showed the highest xylose conversion, with a TOF value of 10.9×10^{-6} $mmol_X$ μmol_{LEWIS}^{-1} h^{-1}. The TOF values, based only on the Lewis sites, of the rest of the catalysts were as follows: 6.5, 8.1 and 4.3×10^{-6} $mmol_X$ μmol_{LEWIS}^{-1} h^{-1} for M-57, M-71 and M-87, respectively. However, as observed in Table 1, the presence of OH groups (as Brønsted) reduced the xylose dehydration activity, and thus reduced the TOF values (calculated based on the total acidity of the fresh catalysts) for all the catalysts except for M-40. The double dosing in

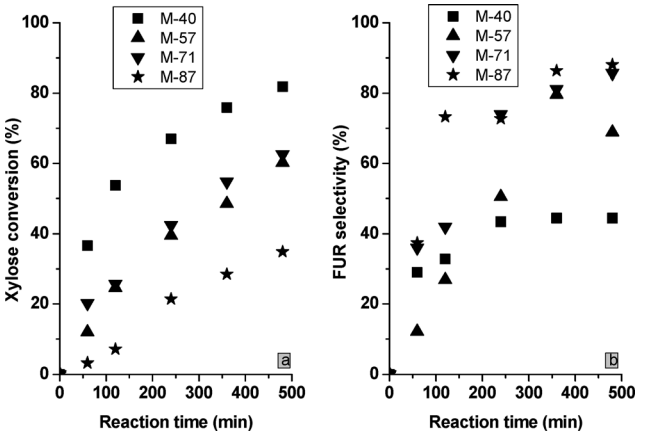

Fig. 4 The evolution of (a) the conversion of xylose and (b) the selectivity to FUR *versus* reaction time during the xylose dehydration tests of the partially hydroxylated sample series at 160 °C in water–toluene.

weight of the catalysts would presumably double the TOF values as well. Among the rest of the catalysts, M-87 showed surprisingly low xylose conversion values. Although this sample exhibited higher total acidity measured by NH_3-TPD, its lower Lewis acid-site content may lead to lower xylose conversion rates. On the other hand, it must be pointed out that the xylose conversion values of M-57 and M-71 had very slight differences.

In order to evaluate the effect of MgF_2 catalysts on the activity (xylose conversion and furfural selectivity), experiments without any catalyst were also carried out. These tests showed a xylose conversion of 23% and a furfural selectivity of 21% (yield of 5% after 8 h of reaction) at 160 °C in water–toluene, confirming the presence of MgF_2 catalysts to improve furfural production.

When bifunctional L + B catalysts such as MgF_2 are in contact with xylose, competitive reactions occur and the reaction rates showed clear differences compared to pure Brønsted acids, such as homogeneous H_2SO_4[14] or Amberlyst.[27] As observed in Fig. 4b, it clearly proved that catalysts containing lower L/B ratios than M-40 could significantly improve the FUR production selectivity (FUR_S). In these cases, the reactions were catalyzed by a combination of Lewis and Brønsted sites, and thus the FUR production shifted to the route showing the highest FUR_S (B_2 route). In general, it was observed that catalysts presenting high L/B ratios (such as 10.9 for M-40) reduced the furfural production yield. On the contrary, by reducing this ratio to 3.6 (for M-87), FUR_S values could be considerably increased. However, the optimum L/B ratio was found for the M-71 catalyst, showing intermediate Lewis acidity and higher OH concentration than M-40 or M-57, thus increasing the FUR yield values.

As reported for other pure Brønsted catalysts, the FUR_S plots present a maximum at the beginning of the reaction, which then drops along the reaction path due to side-reactions.[27] In the MgF_2 system used in this work, however, the presence of intermediates (such as xylulose, evidenced in Fig. A2, ESI† and quantified as represented in Fig. A3, ESI†) reduced the initial FUR selectivity whilst xylulose can be dehydrated and thus the FUR_S increased all along the tests (Fig. 4b). Moreover, as observed in Fig. 4b, the FUR_S decayed after 6 h of reaction for the M-57 sample. Even if xylulose was quantified at this point, FUR side-reactions were enhanced at this point, leading to lower FUR yield values.

Another important reaction parameter was the acid-site density, measured as total acid sites per surface area, showing the following trend: 1.1, 1.5, 0.7 and 0.6 μmol m^{-2} for M-40, M-57, M-71 and M-87, respectively. The higher FUR_S observed for M-71 and M-87 could also result from a lower acid-site density, together with an optimized L/B ratio for furfural production (Table 1). Taking into account that the loss of FUR_S is directly attributed to the side-reactions, such as resinification, higher acid-site densities could enhance these reactions with samples such as M-57. On the other hand, the lower FUR_S observed for M-40 was directly attributed to the low protonation capacity of the weak Brønsted acid sites on its surface (nearly insignificant) or for the reaction medium H_3O^+.

As observed in Table 1, even if the M-87 sample showed the highest FUR_S values, its low xylose conversion values considerably reduced the furfural yield (FUR_Y). In general, the catalyst showing the highest selectivity (M-71) also showed the highest furfural yield values, even after 20 h of reaction. As previously described, furfural yield values strongly depend on the nature and amount of acid-sites. Lewis sites increase xylose conversion values but reduce the FUR selectivity and consequently the yield values. On the contrary, xylose conversion rates are lower for Brønsted sites but yield values are compensated due to higher selectivity values.

Based on the xylose conversion data, the differences were mainly attributed to the change of the reaction mechanism in the presence of Lewis or Brønsted sites. The presence of xylulose (evidenced by the ^{1}H-NMR spectra as shown in Fig. A2, ESI† and quantified as shown in Fig. A3, ESI†) during the reactions showed that Lewis sites catalyzed the xylose conversion to its isomer (L_1) by C═O rearrangement,[34] whilst the presence of Brønsted sites (B_1) was required to further dehydrate xylulose to FUR (Scheme 1).[15] On the other hand, xylose can be directly dehydrated to FUR in the presence of a strong Brønsted site (B_2). A plausible mechanism for the direct xylose-to-furfural reaction consists of transforming the hydroxyl groups of the pentose to H_2O^+ and the elimination of two 1,2 and one 1,4 water molecules.[3,14] In this case, samples such as M-57, M-71 or M-87 could produce FUR *via* L_1 + B_1 or *via* B_2 routes (due to their relatively low L/B ratio). However, dehydration reactions using M-40 could only be catalyzed by weaker Brønsted acid species, *i.e.* the H_3O^+ ions in the reaction medium. As reported, the B_2 route increases the FUR_S, but the overall conversion rate is slower than the L_1 + B_1 route.[15] These reactions were embraced as a general k_1' in Scheme 1. Moreover, the FUR can also be degraded by condensation reactions with fragments (k_2') or

produce FUR resins under the presence of strong acids (k_3'), mainly Brønsted.

According to the ^{1}H-NMR spectra xylulose was present as the only intermediate. As reported in the literature, when Lewis catalysts are present xylulose appears as the only intermediate for furfural production. On the other hand, catalysts showing more Bronsted sites show also the direct xylose conversion route. In this case, as the M-71 catalyst also presented Lewis sites, it also showed the presence of xylulose in the reaction solution.

In order to identify the possible reaction by-products, the soluble phase was analyzed by means of ^{1}H-NMR. Taking into account the low xylose concentration detected and its slow dehydration to furfural,[35] it seemed that xylose was favorably isomerized to xylulose (see Fig. A2, ESI†) under the presence of partially hydroxylated MgF_2 catalysts. The combination of Lewis sites (M-40) and weak Brønsted (H_3O^+) can also convert the pentose carbohydrates to fragments such as formic acid (8.4 ppm, derived from the O_3 protonation[36]), glycolaldehyde (2.2/3.2 ppm) or dihydroxyacetone (4.4 ppm) by retro-aldol reactions (RA). Moreover, other side-products might be derived from the dehydration reactions of xylose/xylulose or from dihydroxyacetone to pyruvaldehyde (2.33 ppm), as well as several other minor fragments at 2.1–2.5 ppm. A detailed characterization and quantification of all the sub-products during reaction is very difficult. Moreover, the presence of humins and coke-deposits makes a detailed carbon balance analysis difficult.

Concerning the effect of the solvent on the activity data, efficient FUR isolation is required to increase the FUR_S. In this sense, the xylose conversion rate of the MgF_2 catalysts only changed slightly under monophasic conditions in water, but showed lower FUR_S values (M-40: 26%, M-57: 33%, M-71: 42% and M-87: 44%). However, the use of an aprotic solvent such as DMSO (a Lewis base with a pK_a of 35) induced significant changes. As observed in Fig. 5, X_X values stopped below 60% after 4 h. Even if the Lewis site might be partially suppressed, M-40 showed again the highest activity. The behavior of M-87 was the only different one compared to water–toluene data. This could be attributed to its very low L/B ratio. However, the FUR_S obtained in DMSO (10%) were below the ones obtained in water.

3.2.2 Effect of glucose addition to xylose feed under batch conditions. According to the data published using xylose and glucose feed (X + G), the xylose and furfural condensation reactions were enhanced in the presence of a second carbohydrate.[26] The kinetic activity of the partially hydroxylated MgF_2 catalysts was also evaluated using 1 : 1 w/w X : G feed at 160 °C in water–toluene. As observed in Fig. 6a, the presence of glucose slightly increased the X_X compared to the one measured with just the X feed for the tests using M-71. Moreover, the conversion of glucose took place at slower catalytic rates. During the X + G tests, the most significant changes were observed for the FUR_S at 160 °C in water–toluene (Fig. 6b). The FUR condensation reactions with glucose and HMF intermediates were

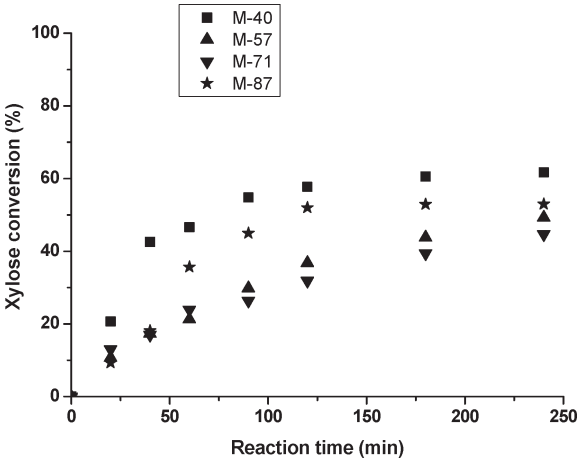

Fig. 5 The reaction time *vs.* xylose conversion of the partially hydroxylated sample series at 160 °C in DMSO.

enhanced[26] and FUR_S reduced from 44 to 38% for M-40 and from 86 to 81% for M-71 after 20 h of reaction in water–toluene. The tests at 180 °C using X + G feed showed a slightly lower FUR_S and a considerable HMF_S decrease (Table 2). When the FUR is not quickly isolated from the reaction medium under batch conditions, the resinification effects could considerably reduce the FUR and HMF selectivities. Given the "high" L/B ratio of these MgF_2 catalysts, this effect was less important than in processes operated with higher Brønsted content. On the other hand, the "entropy effects" related to higher-temperatures[27] showed no effects on the FUR_S.

3.2.3 Study of glucose dehydration to HMF. Research articles, using glucose as a source, reported high HMF yields using metal chlorides[19] or metal oxides[37] under biphasic conditions and zeolites in ionic-liquids.[38] Most of the research studies used fructose, since it shows the highest selectivity to HMF. These processes can avoid the first isomerization reaction (from glucose to fructose) and thus increase the HMF_S up to 72%.[39] However, the high glucose content in the lignocellulosic biomass requires further studies using glucose as the starting feedstock.

This study aims to provide a real solution to the carbohydrate fractions present in the biomass. In this sense, catalysts such as MgF_2, containing Lewis and Brønsted sites, show interesting properties to isomerize the glucose to fructose and dehydrate fructose to HMF *via* Brønsted acid-sites.

The tests at 160 °C performed in water–toluene confirmed the low extraction efficiency of toluene, showing HMF_S of 40% for M-71 (Table 2). The tests carried out at 180 °C slightly increased the HMF_S to 45% for M-71. On the other hand, the use of 1-butanol as a co-solvent, which can also be obtained through the fermentation of biomass derived carbohydrates, considerably increased the HMF_S (58% at 160 °C and 66% at 180 °C). The HMF partition coefficient of solvent–water increased from 0.1 to 2.6 for toluene and 1-butanol, respectively. This higher extraction efficiency decelerated the HMF yield-loss reactions, such as rehydration

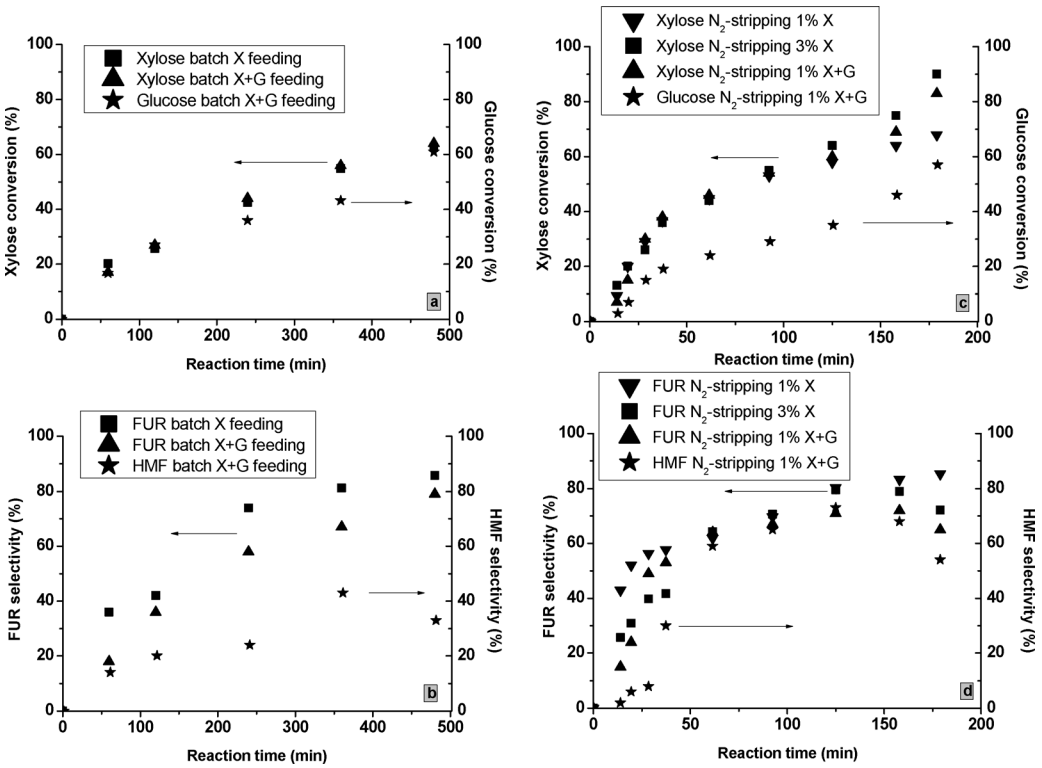

Fig. 6 The xylose and glucose conversions and FUR and HMF selectivities for the tests catalyzed by M-71 under batch conditions at 160 °C in water–toluene (Fig. 6a and b) and N_2-stripping at 180 °C in water (Fig. 6c and d).

Table 2 Xylose conversion and FUR selectivity of different partially hydroxylated MgF_2 catalysts under batch and N_2-stripping at different reaction temperatures

Catalyst	Tests	T (°C)	Feed	X_X[c] (%)	FUR_S[c] (%)	G_X[c] (%)	HMF_S[c] (%)	TOF 10^{6}[e] ($mmol_{X-G}$ μmol_{ACID}^{-1} h^{-1})
M-40	Water–toluene[a]	160	X	82	44	—	—	10.9
M-71				94	86	—	—	6.3
M-71-R_1				98	59			8.1
M-71-R_2				82	52			6.2
M-40	Water–toluene[a]	180	X	90	47	—	—	13.4
M-71				99	75	—	—	8.5
M-40	Water–toluene[a]	160	G	—	—	99	23	11.6
M-71				—	—	85	39	6.1
M-71		180	G	—	—	92	45	9.4
M-71	Water–1-butanol[a]	160	G	—	—	78	58	3.5
M-71		180		—	—	99	66	9.1
M-40	Water–toluene[a]	160	X + G	99	38	99	28	11.2
M-71				97	81	88	40	6.9
M-71	Water–toluene[a]	180	X + G	99	73	99	12	9.3
M-71	N_2-stripping[b,d]	160	X (1%)	64	59	—	—	—
		180	X (1%)	68	87	—	—	—
			X (3%)	90	73	—	—	—
			X + G (1%)	83	65	58	53	—
			X + G (3%)	91	59	82	35	—

[a] Batch tests performed with a 1/1 v/v water/solvent ratio. [b] N_2-stripping performed using 150 mL min^{-1} of N_2 and pressure calculated according to the corresponding vapor pressure. [c] Xylose (X_X) or glucose (G_X) conversion, FUR selectivity (FUR_S) and HMF selectivity (HMF_S) after 20 h of reaction. [d] Xylose conversion for the N_2-stripping tests after 3 h of reaction. [e] Turnover frequency for xylose or glucose after 4 h of reaction and for xylose using the X + G feed. SD: overall standard deviation: ~6%.

to levulinic acid and formic acid and the formation of condensation products.[39] Thus, the combination of suitable reaction solvents and partially hydroxylated MgF_2 seemed promising to optimize the production of HMF from glucose.

3.3 Stability and regenerability of the MgF_2 catalysts under batch conditions

The stability of the catalysts was evaluated in terms of structure and acidity. According to the textural properties of the used catalysts, due to morphological changes all the catalysts suffered a strong decrease of S_{BET} (from 460 to 150 $m^2\ g^{-1}$ for M-71), whilst the pore size increased from 26.9 to 54.8 Å for M-71. The explanation for the decrease of the surface area and the reduction of the pore size is a similar phenomenon as explained in section 3.1.1 for the fresh catalysts. The catalysts prepared using higher water/HF ratios created bigger particle aggregates, and thus these materials showed a decrease of the BET surface area and an increase of the pore size. In the same manner, the experimental tests were carried out in water-phase. Moreover, the conditions were harsher (160 °C) than the fresh sample synthesis conditions (80 °C). This way, M-71 also suffered a similar decrease of the surface area and an increase of the pore size due to the formation of bigger aggregates. This was strictly related to the physical properties of the MgF_2 partially hydroxylated materials. In order to produce structurally stable MgF_2 catalysts under hydrothermal conditions, further work is required in this field. Moreover, according to the liquid ^{19}F-NMR analyses (Fig. A1, ESI†), no fluorinated species were found, proving the stability of the MgF_2 catalyst.

On the other hand, the stability of the acid-sites was determined to evaluate the long-term feasibility of the heterogeneous catalysts, especially concerning their industrial application. The catalysts used during the catalytic tests (using X feed) showed a brown color derived from deposited coke or humins. According to previous studies, the catalysts could be efficiently regenerated by calcination at 280 °C.[40] This allowed avoidance of any interference of the coke on the acidity analyses. However, the coke on MgF_2 catalysts could not be removed at this temperature. Moreover, given the limited thermal stability of the acid-sites, milder oxidation procedures using H_2O_2 on the MgF_2 catalysts were further researched.[41] In a typical regeneration step, 2 g of as-recovered catalysts were treated with 20 g of 30% H_2O_2 at 100 °C in Teflon-lined flasks under severe stirring for 4 h. The materials were filtered, washed with ethanol and dried at 100 °C. The CHN elemental analyses of the treated M-71 proved that 98% of the coke layer could be efficiently removed. According to the Pyr-NMR data, the M-71 sample preserved 80% of its total acidity. This acidity was mainly attributed to the Lewis sites, which corresponded to 78% of the acid-sites on fresh M-71. The type of acidity was also checked by 150-Pyr, showing a strong decay of mostly Brønsted acidity. This fact proved that Lewis sites were more stable than Brønsted under hydrothermal conditions. Apparently, the leaching of the surface hydroxyl groups was enhanced in water at 160 °C. According to the acidity data on used catalysts calcined at 300 °C, only 57% of the total acid-sites were recovered after the calcination treatment.

The regenerated catalysts were further tested at 160 °C in water–toluene (see Table 2). Given the change of the acid-properties of a sample containing more Lewis sites and the decrease of total acidity, the TOF value of the catalyst regenerated in the first run (M-71-R_1) increased from 6.3 to 8.1×10^{-6} $mmol_X\ \mu mol_{ACID}^{-1}\ h^{-1}$. A second run showed even lower acid-content, which decreased the xylose conversion activity. As expected, an increase of the L/B ratio had an opposite effect on the FUR production, reducing the FUR_S from 86% to 59 and 52% for fresh M-71, M-71-R_1 and M-71-R_2, respectively. Given the low catalyst amount used in each test (0.4 g) and the loss on reactor walls and filtration in each regeneration step, additional regeneration tests could not be carried out.

3.4 N_2-stripping of furfural

The current FUR manufacturing process uses between 16 : 1 (Quaker Oats) and 30 : 1 (Rosenlew) steam to product weight ratio.[3] The high energy requirements, the separation stages and the use of homogeneous catalysts make this process environmentally unsustainable. The use of N_2 as the stripping agent could improve the manufacturing process by reducing the heating costs and it can be easily separated and recycled from the stripped stream due to its high volatility.

3.4.1. N_2-stripping using xylose feed. Based on the batch activity results, M-71 was chosen as the most appropriate catalyst for the N_2-stripping tests since it showed the highest FUR yield. During the tests at 160 °C, the xylose dehydration activity of M-71 was not high enough to compensate the reduction of the liquid volume. During the N_2-stripping carried out in the configured set-up, the liquid volume was extracted at a flow of ~7 mL^{-1} min. In this case, the volume reduction was not compensated by the xylose conversion to achieve a constant xylose concentration profile in the reactor during 3 h of reaction. For this reason, higher xylose concentrations increased the condensation reactions and thus reduced the final FUR_S to 59% using an initial xylose concentration (X_0) of 1 wt.% (Table 2). However, the tests carried out at 180 °C using X as the feed considerably increased the FUR_S (87%) compared to other pure non-structured Brønsted catalysts.[27] Taking into account that the xylose concentration was maintained at a similar concentration (1 wt.%) during the N_2-stripping tests, the catalyst to xylose ratio increased and thus xylose conversion at 180 °C increased compared to those in the batch tests (Fig. 6a and c). As expected, the increase of X_0 also accelerated the dehydration and degradation reactions of xylose and FUR. As depicted in Fig. 6d, the FUR_S also showed an increasing trend along the tests. This confirmed again the presence of intermediates such as xylulose, achieving lower initial FUR_S than Brønsted sites but the N_2-stripping experiments showed the highest FUR_S values by the end of the tests. The final FUR_S values for X_0 of 1 and 3 wt.% were 87 and 73%, respectively. The GC-MS analyses of the stripped condensate streams showed high FUR selectivity (nearly 97%). Even if FUR_S using toluene as a co-solvent showed higher values at 160 °C, the separation of by-products and FUR from toluene might show higher purification costs than using the N_2–water–FUR system.

3.4.2 N_2-stripping using xylose + glucose feed. As proved in section 3.2.2, the presence of glucose and HMF accelerated the FUR degradation reactions. In the N_2-stripping tests, this effect could not be avoided either. FUR is more volatile than HMF, so the water–HMF equilibrium showed an inverse effect on the water–FUR, which showed a higher FUR concentration in the stripped phase than in the liquid phase. As observed in Fig. 6d, the selectivity at low X feed (1% X) did not decay by the end of the tests. However, the degradation reactions led to a drop in FUR_S for the X + G feed. As observed in Table 2, the use of N_2 as the stripping agent increased the HMF_S at 180 °C compared to under biphasic water–toluene conditions. The FUR was continuously stripped and HMF could be accumulated in the liquid phase to achieve a selectivity of 53%. Moreover, the kinetics of glucose conversion catalyzed by M-71 was significantly reduced compared to xylose. These two features confirmed that FUR could be continuously extracted in the stripped phase whilst HMF and the remaining glucose could be recovered from the liquid phase. Despite the presence of Lewis sites on the MgF_2 samples and consequently the potential to lower the FUR selectivity, M-71 showed higher FUR and HMF selectivities than non-structured pure Brønsted catalysts, such as Amberlyst 70.[26]

The developed system in this study allowed selective production of FUR and HMF from xylose and glucose, respectively. Future environmentally sustainable processes could upgrade these furan derivatives to higher value-added compounds, such as methyltetrahydrofuran[42] or dimethylfuran.[39]

4. Conclusions

Partially hydroxylated MgF_2 catalysts showed high activity during the dehydration of pentoses and hexoses to furanic aldehydes. The bifunctional properties of the MgF_2 catalysts allowed tuning of the Lewis/Brønsted acid ratio and thus control of the parallel reactions. FUR selectivity could be maximized up to 86% at 160 °C in water using toluene as a co-solvent. When glucose was used as a feed source, high HMF selectivity (66%) could be achieved using 1-butanol as an extracting agent. In general, Brønsted sites were required to achieve high FUR and HMF selectivities. The industrial application and sustainability of the batch process in water–solvent is quite limited. The tests catalyzed by MgF_2 in combination with simultaneous N_2-stripping showed that a FUR selectivity of 87% could be achieved using low xylose concentrations. The combination of xylose + glucose feed showed that high FUR and HMF selectivities could still be achieved. Moreover, the catalysts regenerated by H_2O_2 showed high activity during the dehydration tests in water–toluene at 160 °C. In general, this work proved that partially hydroxylated catalysts show high activity to convert xylose to furfural. Moreover, the N_2-stripping tests showed several advantages with respect to biphasic systems, such as higher product purity and selectivity and thus reduced separation stages. As described throughout this work, the design of an appropriate MgF_2 catalyst and the use of N_2-stripping proved that more sustainable chemical technologies could be developed to achieve environmentally friendly chemical industrial technologies and processes.

Acknowledgements

This work was supported by funds from the Spanish Ministerio de Economía y Competitividad (CTQ-2012-38204-C03-03) and from the Gobierno Vasco (Programa de Formación de Personal Investigador del Departamento de Educación, Universidades e Investigación). The graduate school "fluorine as key element" GRK 1582 founded by the Deutsche Forschungsgemeinschaft DFG is gratefully acknowledged. The authors thank Dr. M. Feist for performing thermal analysis measurements and S. Bäßler for NH_3-TPD and Pyr-adsorption measurements.

Notes and references

1 R. Karinen, K. Vilonen and M. Niemelä, *ChemSusChem*, 2011, **4**, 1002.
2 A. S. Mamman, J. M. Lee, Y. C. Kim, I. T. Hwang, N. J. Park, Y. K. Hwang, J. S. Chang and J. S. Hwang, *Biofuels, Bioprod. Biorefin.*, 2008, **2**, 438.
3 K. J. Zeitsch, in *Sugar Series*, Elsevier, The Netherlands, 1st edn, 2000, vol. 13, p. 1.
4 A. S. Dias, M. Pillinger and A. A. Valente, *J. Catal.*, 2005, **229**, 414.
5 S. Lima, P. Neves, M. M. Antunes, M. Pillinger, N. Ignatyev and A. A. Valente, *Appl. Catal., A*, 2009, **363**, 93–99.
6 I. Agirrezabal-Telleria, J. Requies, M. B. Güemez and P. L. Arias, *Appl. Catal., B*, 2012, **115–116**, 178.
7 A. S. Dias, S. Lima, M. Pillinger and A. A. Valente, *Catal. Lett.*, 2007, **114**, 151.
8 A. S. Dias, S. Lima, M. Pillinger and A. A. Valente, *Carbohydr. Res.*, 2006, **341**, 2946.
9 A. S. Dias, S. Lima, P. Brandao, M. Pillinger, J. Rocha and A. A. Valente, *Catal. Lett.*, 2006, **108**, 179.
10 S. B. Kim, S. J. You, Y. T. Kim, S. Lee, H. Lee, K. Park and E. D. Park, *Korean J. Chem. Eng.*, 2011, **28**, 710.
11 C. Moreau, R. Durand, D. Peyron, J. Duhamet and P. Rivalier, *Ind. Crops Prod.*, 1998, **7**, 95.
12 A. Chareonlimkun, V. Champreda, A. Shotipruk and N. Laosiripojana, *Bioresour. Technol.*, 2010, **101**, 4179.
13 G. H. Jeong, E. G. Kim, S. B. Kim, E. D. Park and S. W. Kim, *Microporous Mesoporous Mater.*, 2011, **144**, 134.
14 M. J. Antal, T. Leesomboon, W. S. Mok and G. N. Richards, *Carbohydr. Res.*, 1991, **217**, 71.
15 V. Choudhary, A. B. Pinar, S. I. Sandler, D. G. Vlachos and R. F. Lobo, *ACS Catal.*, 2011, **1**, 1724.
16 R. Weingarten, G. A. Tompsett, W. C. Conner and G. W. Huber, *J. Catal.*, 2011, **279**, 174.
17 S. Lima, A. Fernandes, M. M. Antunes, M. Pillinger, F. Ribeiro and A. A. Valente, *Catal. Lett.*, 2010, **135**, 41.
18 S. Lima, M. M. Antunes, A. Fernandes, M. Pillinger, M. F. Ribeiro and A. A. Valente, *Appl. Catal., A*, 2010, **388**, 141.
19 Y. J. Pagán-Torres, T. Wang, J. M. R. Gallo, B. H. Shanks and J. A. Dumesic, *ACS Catal.*, 2012, **2**, 930.

20 Y. R. Leshkov, M. Moliner, J. A. Labinger and M. E. Davis, *Angew. Chem., Int. Ed.*, 2010, **49**, 8954.
21 S. B. Troncea, S. Wuttke, E. Kemnitz, S. M. Coman and V. I. Parvulescu, *Appl. Catal., B*, 2011, **107**, 260.
22 E. Kemnitz, S. Wuttke and S. M. Coman, *Eur. J. Inorg. Chem.*, 2011, 4773.
23 S. Wuttke, S. M. Coman, G. Scholz, H. Kirmse, A. Vimont, M. Daturi, S. L. M. Schroeder and E. Kemnitz, *Chem.–Eur. J.*, 2008, **14**, 11488.
24 I. Agirrezabal-Telleria, F. Hemmann, C. Jäger, P. L. Arias and E. Kemnitz, *J. Catal.*, 2013, **305**, 81.
25 Q. Jing and X. Y. Lu, *Chin. J. Chem. Eng.*, 2007, **15**, 666.
26 I. Agirrezabal-Telleria, J. Requies, M. B. Güemez and P. L. Arias, *Green Chem.*, 2012, **14**, 3132.
27 I. Agirrezabal-Telleria, A. Larreategui, J. Requies, M. B. Güemez and P. L. Arias, *Bioresour. Technol.*, 2011, **102**, 7478.
28 D. G. Cory and W. M. Ritchey, *J. Magn. Reson.*, 1988, **80**, 128.
29 F. Hemmann, G. Scholz, K. Scheurell, E. Kemnitz and C. Jaeger, *J. Phys. Chem. C*, 2012, **116**, 10580.
30 D. M. Grant and R. K. Harris, *Encyclopedia of Nuclear Magnetic Resonance*, John Wiley & Sons Ltd., Chichester, U. K., 1996, vol. 5, p. 3247.
31 D. A. Torchia, *J. Magn. Reson.*, 1978, **30**, 613.
32 G. Scholz, C. Stosiek and E. Kemnitz, *J. Fluorine Chem.*, 2011, **132**, 1079.
33 A. Onda, T. Ochi and K. Yanagisawa, *Green Chem.*, 2008, **10**, 1033.
34 J. Mikkola, R. Sjöholm, T. Salmi and P. Mäki-Arvela, *Catal. Today*, 1999, **48**, 73.
35 R. O'Neill, M. N. Ahmad, L. Vanoye and F. Aiouache, *Ind. Eng. Chem. Res.*, 2009, **48**, 4300.
36 M. R. Nimlos, X. H. Qian, M. Davis, M. E. Himmel and D. K. Johnson, *J. Phys. Chem. A*, 2006, **110**, 11824.
37 J. H. Zhang, L. Lin and S. J. Liu, *Energy Fuels*, 2012, **26**, 4560.
38 H. Jadhav, E. Taarning, C. M. Pedersen and M. Bols, *Tetrahedron Lett.*, 2012, **53**, 983.
39 Y. Román-Leshkov, J. N. Cheda and J. A. Dumesic, *Science*, 2006, **312**, 1933.
40 I. Agirrezabal-Telleria, J. Requies, M. B. Güemez and P. L. Arias, *Appl. Catal., B*, 2014, **145**, 34.
41 X. Shi, Y. Wu, H. Yi, G. Rui, P. Li, M. Yang and G. Wang, *Energies*, 2011, **4**, 669.
42 J. P. Lange, E. van der Heide, B. van Buijtenen and R. Price, *ChemSusChem*, 2012, **5**, 150.

